ACS SENSORS

Article

Cite This: ACS Sens. 2019, 4, 1399−1408

pubs.acs.org/acssensors

# Label-Free Surface Protein Profiling of Extracellular Vesicles by an Electrokinetic Sensor

Sara Cavallaro,[†] Josef Horak,[‡] Petra Håag,[§] Dhanu Gupta,[∥,#] Christiane Stiller,[‡] Siddharth S. Sahu,[⊥] André Görgens,[∥,#,▽] Hithesh K. Gatty,[⊥] Kristina Viktorsson,[○] Samir El Andaloussi,[∥,#] Rolf Lewensohn,[○] Amelie E. Karlström,[‡] Jan Linnros,[†] and Apurba Dev*[,⊥]

[†]Department of Applied Physics, School of Engineering Sciences, KTH Royal Institute of Technology, 16440 Kista, Sweden

[‡]Department of Protein Science, School of Engineering Sciences in Chemistry, Biotechnology and Health, KTH Royal Institute of Technology, AlbaNova University Center, 10691 Stockholm, Sweden

[§]Department of Oncology/Pathology, Karolinska Institutet, Karolinska University Hospital (Theme, Cancer; Patient Area, Pelvis), Akademiska stråket 1, 171 64 Solna, Stockholm, Sweden

[∥]Clinical Research Center, Department of Laboratory Medicine, Karolinska Institutet, 171 77 Stockholm, Sweden

[⊥]Department of Solid State Electronics, The Ångström Laboratory, Uppsala University, Box 534, Uppsala SE-751-21, Sweden

[#]Evox Therapeutics Limited, Oxford OX4 4HG, United Kingdom

[▽]Institute for Transfusion Medicine, University Hospital Essen, University of Duisburg-Essen, 45122 Essen, Germany

[○]Department of Oncology/Pathology, Karolinska Institutet, Karolinska University Hospital (Theme, Cancer; Patient Area, Head and Neck, Lung, and Skin), Akademiska stråket 1, 171 64 Solna, Stockholm, Sweden

*Supporting Information*

**ABSTRACT:** Small extracellular vesicles (sEVs) generated from the endolysosomal system, often referred to as exosomes, have attracted interest as a suitable biomarker for cancer diagnostics, as they carry valuable biological information and reflect their cells of origin. Herein, we propose a simple and inexpensive electrical method for label-free detection and profiling of sEVs in the size range of exosomes. The detection method is based on the electrokinetic principle, where the change in the streaming current is monitored as the surface markers of the sEVs interact with the affinity reagents immobilized on the inner surface of a silica microcapillary. As a proof-of-concept, we detected sEVs derived from the non-small-cell lung cancer (NSCLC) cell line H1975 for a set of representative surface markers, such as epidermal growth factor receptor (EGFR), CD9, and CD63. The detection sensitivity was estimated to be ∼175000 sEVs, which represents a sensor surface coverage of only 0.04%. We further validated the ability of the sensor to measure the expression level of a membrane protein by using sEVs displaying artificially altered expressions of EGFR and CD63, which were derived from NSCLC and human embryonic kidney (HEK) 293T cells, respectively. The analysis revealed that the changes in EGFR and CD63 expressions in sEVs can be detected with a sensitivity in the order of 10% and 3%, respectively, of their parental cell expressions. The method can be easily parallelized and combined with existing microfluidic-based EV isolation technologies, allowing for rapid detection and monitoring of sEVs for cancer diagnosis.

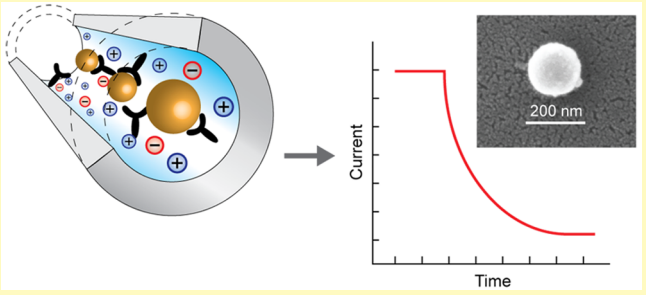


**KEYWORDS:** *extracellular vesicles, electrokinetic effect, biosensor, label-free, protein profiling, cancer*

Recent studies have revealed that extracellular vesicles (EVs) participate in a wide range of physiological processes, such as intercellular communication, tissue repair, and in the regulation of immune response.[1,2] It has also been demonstrated that EVs play a leading role in the pathogenesis of many diseases, including cancer progression.[1−3] Exosomes, a subtype of EVs, have drawn particular interest as a source of biomarkers for cancer diagnosis, because their content reflects their tumor cell of origin and their presence in body fluids enables minimally invasive disease monitoring.[1,2] Although the precise definition is still controversial,[1,4,5] small EVs (sEVs, 40−200 nm in diameter) derived from the endolysosomal pathway and enclosed by a lipid bilayer are usually referred to as exosomes.[1,5] In the context of tumors, investigations during the past decade have discovered the ability of exosomes to stimulate tumor progression and metastasis development, in addition to controlling the communication between tumor

Received: February 28, 2019
Accepted: April 25, 2019
Published: April 25, 2019






DOI: 10.1021/acssensors.9b00418
ACS Sens. 2019, 4, 1399−1408

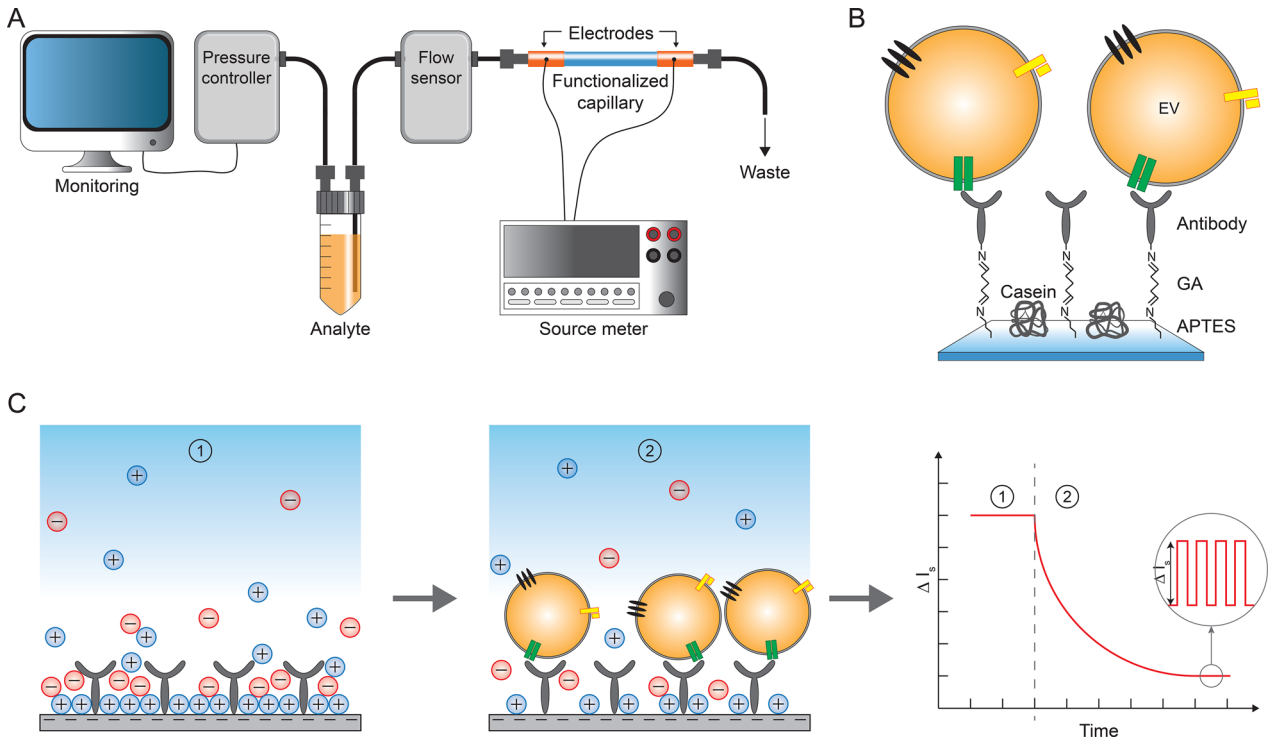


**Figure 1.** Electrokinetic platform and detection principle. (A) Schematics of the measurement setup. (B) Schematics of the inner capillary surface functionalization strategy, showing immobilized antibodies as affinity reagents for capture of sEVs by their surface proteins. (C) Schematics of the electrokinetic detection technique, showing the change in the streaming current difference ($\Delta I_{s2} - \Delta I_{s1}$) between buffer injection (region 1) and sEVs binding to the affinity reagents on the sensor surface (region 2). Inset showing the streaming currents recorded for the periodic pressure pulses of 1.5 and 3 bar, from which $\Delta I_s$ and $\zeta^*$ are calculated and monitored over time. Schematics are not to scale for the sake of simplicity.

cells and the immune system.[2,6,7] An intense interest has therefore developed for exosome-based liquid biopsies, where the tumor and its treatment response can be directly and repeatedly monitored in body fluids,[8,9] e.g., in plasma, pleural effusion, urine, or saliva, unlike traditional tissue-based biopsies. In addition, because exosomes are secreted by early stage tumor cells, liquid biopsies based on exosomal surface markers also offer a promising option for early cancer detection.[10]

The main techniques currently used to detect sEVs involve molecular counting approaches, e.g., dynamic light scattering;[11] conventional antibody-based immunoassays,[12−15] e.g., flow cytometry;[12] or optical methods,[16−21] e.g., surface plasmon resonance (SPR). A large number of microfluidic-based technologies are also available for both isolation and/or detection. These include deterministic lateral displacement arrays (DLDs), microfluidic-based membrane filtration, microfluidic-based immunoaffinity capture, ExoChip, and fluorescence flow cytometer, etc.[21−24] These methods have been described and compared in a number of review articles.[23,25,26] Despite the good performances and advantages in their specific uses, some of these methods are limited by a number of factors, such as being time-consuming and employing bulky and expensive detection devices, in addition to requiring large sample volumes and extensive labeling for detection. Others have instead reported on electrical detection of EVs,[27−31] however, all of them employing electrochemical readouts. Moreover, in most of these cases, signal amplification and/or sample enrichment strategies have been employed,[27,29,30] making these approached multisteps and increasing their analytical cost.

In comparison, electrokinetic approaches, widely used for sensitive surface characterization, offer a simple yet efficient method for the determination of molecule deposition kinetics and surface coverage at a solid−liquid interface.[32] Although extensive studies involving a variety of particles, e.g., latex, colloidal gold, or dendrimers, have been reported in the literature,[32] the practical application of the method, particularly in the field of specific biomolecule detection, has been limited to the detection of proteins or small molecules only.[33−35] The theoretical studies, validated by experimental investigations, however, indicate a stronger electrokinetic effect with larger molecules.[36,37] Therefore, sEVs, being 100−1000-fold larger than most proteins, offer a potentially favorable situation for sensitive detection with electrokinetic approaches. Here, for the first time, we demonstrate the prospect of using an electrokinetic method for label-free detection and profiling of sEVs in the size range of exosomes. The method measures the changes in streaming current ($\Delta I_s$) within a functionalized microcapillary upon sEV binding. Moreover, being purely electrical, it does not require any intermediate labeling steps, allowing for direct detection from small sample volumes. At the same time, it offers the possibility of easy integration with microfluidics-based exosome isolation techniques as well as scaling up with simple fabrication steps, illustrating a potential clinical utility for cancer diagnostics and/or therapy monitoring.

To prove the concept, we first demonstrated the detection of sEVs based on a set of representative surface markers, which included the tumor-associated protein epidermal growth factor receptor (EGFR) and the exosomal tetraspanin family proteins CD9 and CD63. For this investigation, the sEV samples were harvested from the non-small-cell lung cancer (NSCLC)



DOI: 10.1021/acssensors.9b00418
ACS Sens. 2019, 4, 1399−1408

H1975 cell line. The target selectivity was achieved by immobilizing target-specific affinity reagents. Furthermore, we evaluated the detection sensitivity, representing the minimum detectable sEV concentration, and reproducibility by a series of measurements. Finally, we analyzed sEV samples containing different expression levels of EGFR and CD63, where the EGFR expression was reduced by siRNA in NSCLC H1975 cells and the CD63eGFP fusion protein was overexpressed by stable transfection in HEK 293T cells. The results showed the prospect of semiquantitative expression profiling of sEV surface markers with high sensitivity and reproducibility.

## MATERIALS AND METHODS

**Reagents.** Ultrapure water was prepared using a Milli-Q synthesis water purification system (Merck Millipore, Germany). Phosphate-buffered saline (PBS) in tablets was purchased from VWR Life Science. Anti-CD9 antibody (ab195422) was purchased from Abcam; anti-CD63 antibody (mab5048), from R&D System. As affinity reagent against EGFR, the affibody $Z_{EGFR:2377}$ was recombinantly produced at the Department of Protein Science at KTH, Sweden[38] (method in the Supporting Information). If not stated otherwise, all of the other chemicals were purchased from Sigma-Aldrich.

**Detection Method.** For the detection, the $I_s$ induced by a pressure driven flow of a PBS buffer (or sample) through a hollow silica microcapillary was measured. All of the experiments were performed with a microcapillary having an inner diameter of 25 $\mu$m and a length of ∼4 cm. Figure 1A shows a schematic representation of the electrokinetic detection setup. A flow sensor (Elveflow, MFS3) placed at the inlet of the microcapillary was used to monitor and maintain the flow rates. A pair of electrodes, a Pt tube at the inlet, and an Ag/AgCl reference electrode at the outlet of the microcapillary were used to measure the streaming current. Using a commercial pumping system (Elveflow, OB1), a continuous train of periodic rectangular pressure pulses (30 s pulse duration) of 1.5 bar pulse height (1.5−3 bar) were generated to drive the solutions through the microcapillary. The flow rates were measured to be 6 and 3 $\mu$L/min for the applied pressures of 3 and 1.5 bar, respectively. The $I_s$ for the periodic pressure pulses was recorded by using a Keithley source meter and then converted to a change in the apparent $\zeta$ potential ($\zeta^*$) according to the following equation:[39]

$$\zeta^* = \frac{\Delta I_s}{\Delta P}\frac{\eta}{\varepsilon\varepsilon_0}\frac{L}{A} \quad (1)$$

where $\frac{\Delta I_s}{\Delta P}$ is the change in $I_s$ with pressure, $\eta$ the viscosity, $\varepsilon\varepsilon_0$ the permittivity, and $L/A$ the length and cross-section of the capillary, respectively. The collected data were analyzed by a custom-designed software.

The inner surface of the microcapillary was functionalized with affinity reagents against specific sEV membrane proteins, immobilized via glutaraldehyde (GA) coupling (Figure 1B). Upon injection, the sEVs gradually diffused to the surface, allowing interaction of their surface proteins with the immobilized affinity reagents. This led to a change in the streaming current, which was directly measured by the setup (Figure 1C). All experiments were performed at room temperature with PBS at pH 7.4. However, the PBS buffer was diluted to 0.1× to decrease the concentration of counterions, thereby increasing the magnitude of the measured $\zeta^*$.[40]

**Surface Functionalization.** The capillary inner surfaces were functionalized following the procedure reported by Dev et al.[33] A detailed description is presented in the Supporting Information.

**sEV Purification and Isolation.** Two different sources of sEVs were used and analyzed in this study. The tumor derived sEVs were collected from the NSCLC H1975 cell line expressing mutant EGFR (*L858R* and *T790M*),[41] whereas the second sEV source was derived from the HEK 293T cell line, engineered to overexpress CD63 fused to eGFP (CD63eGFP). For the NSCLC H1975 sEV isolation, a standard size exclusion chromatography method was used, whereas, for the HEK 293T sEV isolation, a differential centrifugation protocol was followed[12,42] (detailed descriptions in the Supporting Information).

**Ablation of EGFR Expression on NSCLC sEVs.** H1975 cells were plated in 175 $cm^2$ flasks with RPMI-1640 medium supplemented with 10% fetal bovine serum (FBS). The following day, cells were washed with serum-free media and transfected with 50 nM si-EGFR (No. AM51331, Life Technology) or control siNT (No. 12935300, Life Technology) using Dharmafect 1 (Dharmacon) as transfection reagent for about 4 h, followed by addition of 10% FBS. After 24 h, the transfection medium was removed and cells were washed with media containing exosome-depleted serum and grown for another 48 h in exosome-depleted FBS media. sEVs were isolated as described in the Supporting Information. Cells as well as EVs were harvested for RNA and protein analyses.

**sEV Characterization.** The sEV samples from NSCLC H1975 cells were characterized using nanoparticle tracking analysis (NTA), Western blot (WB), qPCR, and scanning electron microscopy (SEM) (methods in the Supporting Information, results in Figure S1). The sEVs derived from HEK 293T cells were characterized by NTA, flow cytometry, and fluorescence microscopy (methods in the Supporting Information, results in Figure S2).[12,43] The stability of both sEV samples used in this study in 0.1 × PBS was evaluated by NTA, which showed insignificant influence from the buffer ionic strength and integrity of the molecules in this buffer (Figure S3).

**Surface Plasmon Resonance on NSCLC sEVs.** Experiments were conducted in a BIAcore 2000 instrument (GE Healthcare) using 1 × PBS, pH 7.4 as a running buffer. Commercial CM5 sensor chips (GE Healthcare) were used. The system was equilibrated with running buffer until a stable baseline was obtained. All capture probes were covalently coupled to the carboxymethylated dextran matrix using the standard EDC/NHS amine coupling procedure, preconcentration 100 mM sodium acetate buffer, pH 4.5, and 10 min contact time at 10 $\mu$L/min. Affibody molecules were immobilized at 40 $\mu$g/mL and antibody molecules at 10 $\mu$g/mL, which resulted in approximately 6000 RU and 12000 RU final immobilization levels against control surface. EV detection and dilution was performed in filtered and degassed running buffer; the analyte was injected at 10 $\mu$L/min for 20 min. The chip surface was regenerated by 10 s injection of 10 mM HCl.

## RESULTS

**Electrical Detection of sEVs and Detection Specificity.** For setting up the device, we selected EGFR as a target marker and used anti-EGFR affibody as an affinity reagent. The rationale for using this protein was that EGFR is frequently mutated and/or overexpressed in different tumor types and is an oncogenic driver in some non-small-cell lung cancers, thereby being a target of oncological clinical relevance.[41,44] Accordingly, the sEVs utilized in these experiments were secreted from the NSCLC H1975 cell line expressing a mutant, constitutively active EGFR. The purified sEV samples were characterized by NTA to estimate their size distribution and particle counts, whereas their morphologies were investigated by SEM. For the analysis of protein expression, WB analysis was used (Figure S1).

For the electrokinetic detection measurements, we recorded $\zeta^*$ as a function of time by first injecting a freshly prepared 0.1 × PBS buffer. This was followed by sEV injection under identical pressure and flow profiles, while recording the association curve. Figure 2A shows a typical real-time response curve of sEVs interacting with immobilized anti-EGFR affibody on the capillary surface. As presented, the sample injection induced a gradual change in $\zeta^*$ and was followed by 0.1 × PBS injection, to remove unbound/loosely bound molecules. However, considering that the bound sEVs may also start dissociating at this stage, a fixed buffer injection period of 30


DOI: 10.1021/acssensors.9b00418
ACS Sens. 2019, 4, 1399−1408

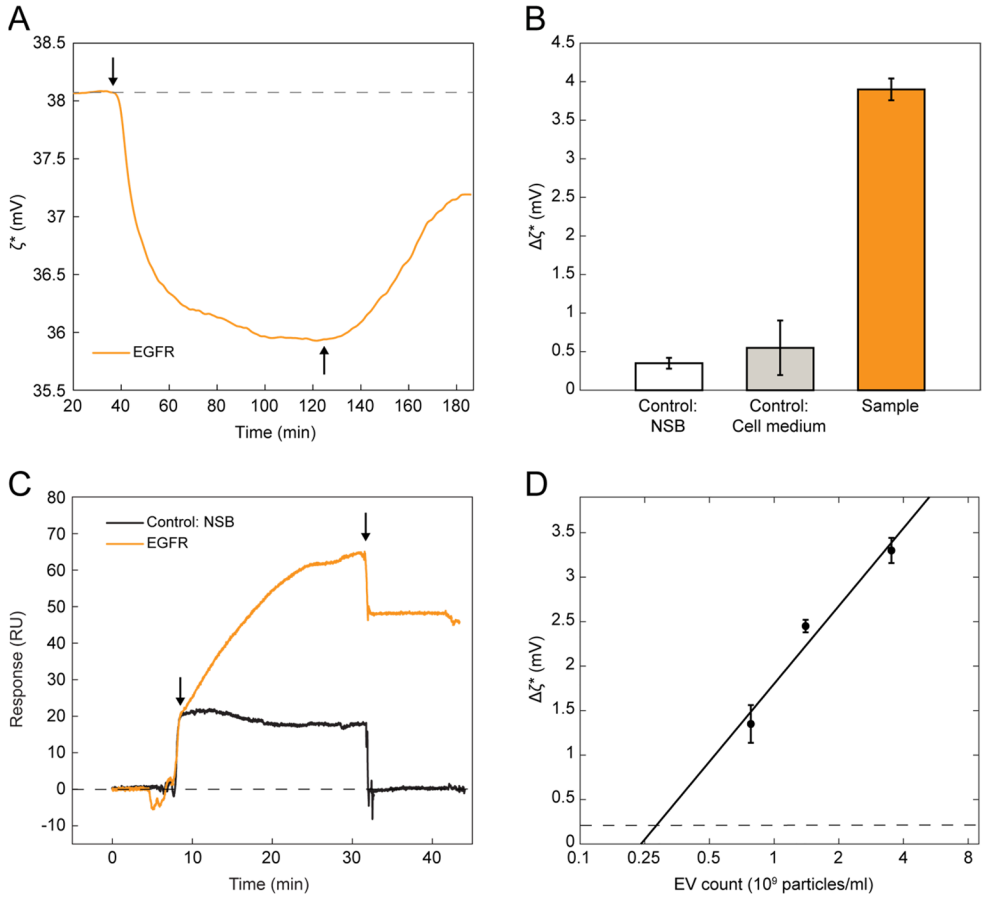


**Figure 2.** Detection of NSCLC H1975 sEVs targeting the EGFR surface marker using an anti-EGFR affibody and specificity of capture. (A) Real-time measurement showing a typical response curve of the electrokinetic microcapillary sensor. sEVs were injected for about 80 min at a concentration of $2 \times 10^9$ particles/mL. Arrows indicate the beginning and end of sEV injection; the dashed line delimits the measured signal. (B) Bar plot showing the typical signal arising from the end-point measurement approach and the sensor responses to control measurements (anti-EGFR affibody capillaries upon sEV-free cell medium injection and capillaries without anti-EGFR affibody upon sEV injection). sEVs were incubated at a concentration of $3.4 \times 10^9$ particles/mL. Measurements performed in triplicate and shown as mean ± SD. (C) SPR response when targeting the same EGFR on sEVs, which were injected at a concentration of $1 \times 10^9$ particles/mL. Arrows indicate the beginning and the end of sEV injection; dashed line delimits the measured signals. Control measurement performed with a functionalized chip without anti-EGFR affibody, to test the influence of NSB. (D) Capillary sensor response showing the signal as a function of the sEV concentration. The dashed line represents the minimum detectable signal. All measurements repeated at least three times, here reported upon control subtraction and displayed as mean ± SD.

min was maintained for all measurements. The signal was then calculated as the difference between the two PBS baselines ($\Delta\zeta^*$). Although such real-time measurements can be used for various kinetic analyses, they may have limited practical use, considering the large sample volumes required (~400 $\mu$L). Hence, for the rest of the investigations presented here, we followed an end-point measurement approach, where the sample was incubated inside the capillary for 2 h. The streaming current in this case was only recorded during the buffer injections. Moreover, during incubation, small sample plugs (~0.5 $\mu$L) were periodically injected (every 5 min) in order to avoid bulk depletion. Unlike the real-time approach, this method only required ~12 $\mu$L of sample for each measurement. The results were then represented as bar plots indicating the $\Delta\zeta^*$ between the two PBS baselines. Figure 2B shows a typical bar plot illustrating the signal arising from different control experiments, as well as specific interaction between the EGFR expressed on the sEVs and the anti-EGFR affibody on the capillary surface. The control measurements were performed in order to estimate both the influence of non-specific binding (NSB) of the sEVs and the cross-reactivity with the sEV-free cell medium[45] (medium supplemented with exosome-depleted FBS and treated as the sEV samples). The NSB was tested by analyzing the sensor response for an identical capillary surface but without immobilized affinity reagents, whereas the influence of cross-reactivity was tested by injecting the sEV-free cell medium in a microcapillary containing immobilized affinity reagents. The comparison presented in Figure 2B clearly shows that the sensor response to the non-specific interactions is insignificant compared to the specific ones. To verify and validate the sensor results with a standard label-free technique, a commercial SPR system was also used to study the same set of interactions and batch of sEV samples (Figure 2C). The results suggested specific sEV detection and a good qualitative agreement with the electrokinetic measurements.

Furthermore, to estimate the minimum measurable concentration, we performed a number of measurements with sEV samples in the concentration range of $(0.78–3.50) \times 10^9$ particles/mL, incubated inside the capillaries for 2 h. These resulted in the calibration curve presented in Figure 2D. The minimum measurable concentration was derived from the



DOI: 10.1021/acssensors.9b00418
ACS Sens. 2019, 4, 1399–1408

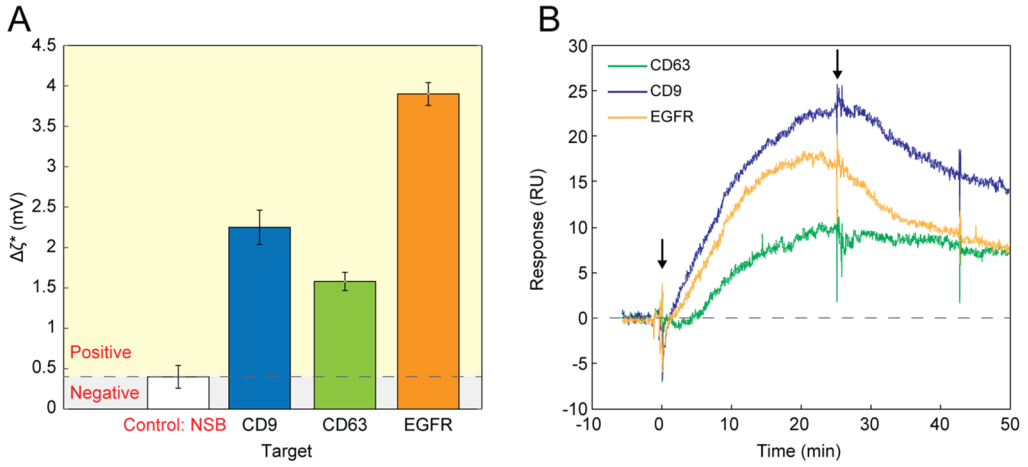


**Figure 3.** Qualitative analysis of surface markers on NSCLC H1975 sEVs, measured at a concentration of $3.4 \times 10^9$ particles/mL, which is within the range of sEV concentrations in plasma samples. (A) Microcapillary biosensor responses for different surface proteins: CD9, CD63, and EGFR. CD9 and CD63 proteins were targeted using anti-CD9 and anti-CD63 antibody functionalized capillaries, respectively. EGFR was targeted using the anti-EGFR affibody. The responses to the specific markers are reported upon cell media control subtraction. The control measurements represented as a white cutoff bar show the influence of NSB. Experiments repeated at least 3 times and shown as mean ± SD. (B) SPR responses validating the specific detection of sEVs when targeting CD9, CD63, and EGFR surface markers. Binding curves represent the response upon NSB control subtraction ($n = 2$).

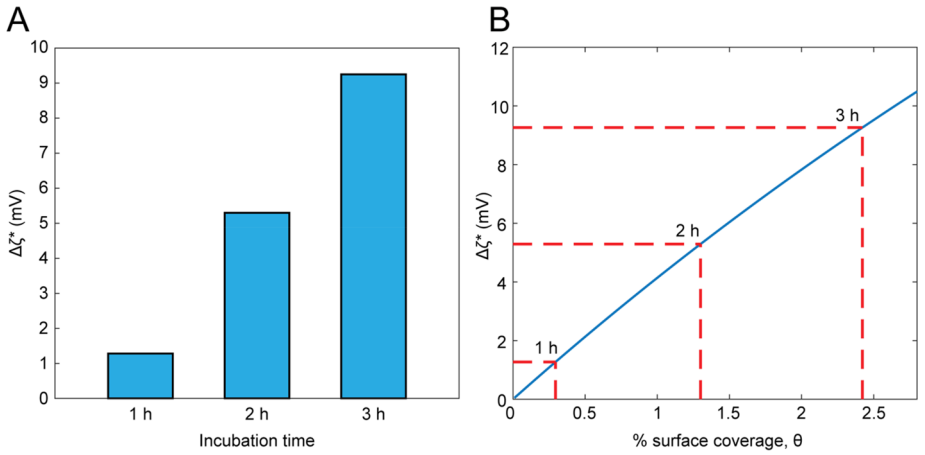


**Figure 4.** Dependence of the electrokinetic sensor response on the NSCLC H1975 sEV incubation time. (A) Sensor response to sEVs targeted against CD9 surface protein using anti-CD9 antibody and injected for 1, 2, and 3 h, respectively. Controls to test the influence of NSB have been subtracted. (B) Variation of the ζ* potential signal with the surface coverage, according to eq S1 in the Supporting Information, for a 98 nm sEV. Red dashed lines indicate the surface coverages for 1, 2, and 3 h sEV incubation corresponding to panel A.

intercept of the calibration curve with the dashed line representing three times the standard deviation (SD) of a blank measurement.[46] In this case, the SD of a blank measurement represents the RMS value of noise in a baseline measurement. The value of 3 × SD in our case was 0.2 mV, which we assigned as the threshold for a reliable measurement. From the extrapolation of the calibration plot, the minimum measurable concentration satisfying the above limit was found to be $2.8 \times 10^8$ particles/mL.

**Multimarker Analysis of sEV Surface Proteins.** It is well-known that the protein composition of sEVs varies between physiological and pathological conditions, as well as cells and tissues of origin,[47] meaning that distinct tumor-derived exosomes express different markers or common markers at altered expression levels. Having validated the efficacy of the electrokinetic technique in detecting sEVs by their surface markers, we applied the method to analyze a panel of their surface proteins. For this purpose, we functionalized the capillaries with specific affinity reagents and measured Δζ* for each biomarker, keeping the sEV concentration identical over all experiments.

Because we mainly worked with sEVs in the size range of exosomes, we screened two tetraspanin family proteins, CD9 and CD63, that are reported to be enriched in this group of sEVs[48,49] (Figure 3A). For easier comparison, we further included the sensor response to the tumor marker EGFR[49] presented in Figure 2B. Clearly, the sensor response displayed a distinct variation in the signal strength for the different surface markers. In particular, the Δζ* for CD63, CD9, and EGFR were found to be 3-, 4.5-, and 8-fold larger than the control experiments (NSB). Given that the measurements were done on the same sample, such a variation in the signal amplitude may be attributed to the differences in the marker interaction affinities or expression levels, or a combination of both. Certainly, from such a study, a direct correlation between the signal strength and the expression levels of the proteins is


DOI: 10.1021/acssensors.9b00418
ACS Sens. 2019, 4, 1399−1408

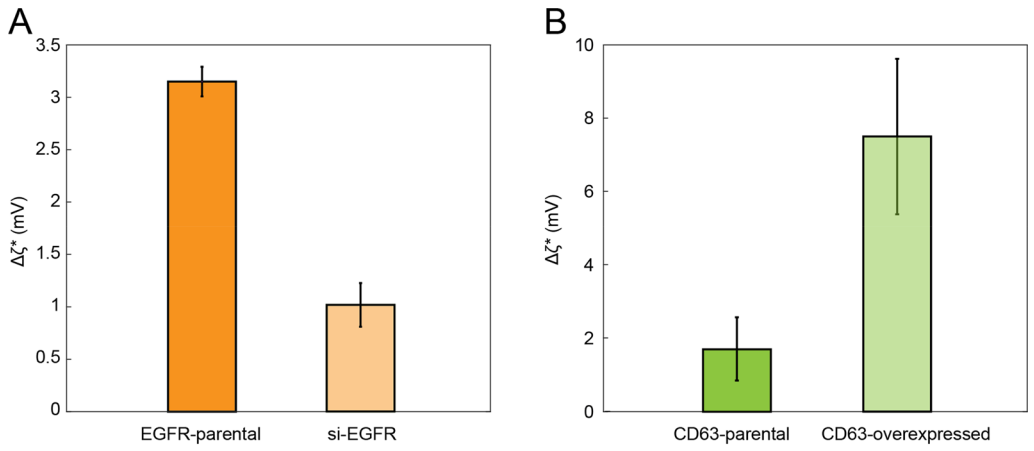


**Figure 5.** Analysis of the sensor response to different surface protein levels. (A) Signal dependence on EGFR expression for NSCLC H1975 sEVs. Sensor responses from anti-EGFR affibody functionalized capillaries upon injection of EGFR-parental and si-EGFR EVs, at a concentration of $3.5 \times 10^9$ particles/mL. (B) Signal dependence on CD63 protein expression for HEK 293T sEVs. Sensor responses from anti-CD63 antibody functionalized capillaries upon injection of CD63-parental and CD63eGFP-overexpressed sEVs, at a concentration of $2.8 \times 10^9$ particles/mL. The responses of both samples to the specific markers are reported upon NSB control subtraction.

difficult to make without the knowledge of their relative interaction affinities and affinity reagent immobilization levels. However, for practical purposes, such measurements can be used for the relative expression analysis of the surface markers, by comparing the signal strength of a given marker between two or multiple sets of EVs, e.g., samples collected from patients at different treatment stages. Such semiquantitative methods of expression analysis are widely used, as evident in the literature.[20,27] The results from the electrokinetic measurements were further verified by SPR (Figure 3B). The difference in the relative signal amplitudes between the electrokinetic sensor and the standard SPR was most likely a consequence of the different affinity reagent immobilization levels on the two substrates. However, SPR data confirmed the presence of the analyzed markers on the EV surfaces, showing good qualitative agreement with our method.

**Detection Time and Sensitivity.** Clearly, the presented sensing principle offers a simple and inexpensive means for direct electrical profiling of EV surface markers. However, in order to understand the physical mechanism limiting the capacity for faster and more sensitive detection, we performed a series of measurements by incubating the sEVs in the capillary for different times. For the analysis, NSCLC-derived EV samples at a concentration of $3.4 \times 10^9$ particles/mL were used against capillaries functionalized with anti-CD9 antibody. The results indicated that the signal increased with incubation time (Figure 4A), as expected for a slow binding rate. At the same time, the data also suggested that even with the highest particle counts used in the entire study, 2 h of incubation did not lead to the maximum signal. The low surface coverage was further theoretically examined by utilizing an existing model, as presented in the Supporting Information (Section S4). Figure 4B shows the calculated $\zeta^*$ as a function of surface coverage estimated for 98 nm sEVs and the predicted surface coverage corresponding to the signal shown in Figure 4A is denoted by the red dashed lines. Clearly, the surface coverage remains very low even after 3 h of sample incubation.

**Expression Analysis of sEV Surface Proteins.** In the context of sensor development for expression analysis of sEV surface markers, perhaps a more appropriate benchmarking parameter is how small a change in the expression level of a target can be reliably detected by the sensor. As discussed in the preceding section, the sensor sensitivity toward the expression level will also depend on the interaction affinity of the targeting probes, and therefore is expected to be different for different protein-affinity reagent pairs. To evaluate the sensitivity of the proposed method in expression analysis, we artificially altered the expression level of two surface markers and measured the sensor response as a function of such altered target expressions. We analyzed the CD63 protein on the sEVs derived from HEK 293T cells and the EGFR on the sEVs derived from NSCLC H1975 cells. Particularly, the CD63 expression in HEK 293T sEVs was enhanced by stable transduction of the parental cells with lentiviral vectors expressing the CD63eGFP fusion, whereas the EGFR expression was reduced by siRNA in the NSCLC H1975 cells (details in Materials and Methods). The selection was motivated by the fact that HEK 293T is the most widely used cell source in engineered EV research, due to its relatively simple culture characteristics and high transfection efficiency, and it could be applied to study the CD63 tetraspanin, which is highly expressed on sEVs. The harvested sEVs from the modified as well as the parental cells were characterized by WB (NSCLC sEVs) and multiplexed bead-based profiling (HEK sEVs, MACSPlex Exosome assay)[12] for semiquantitative assessment of their expression levels (Figures S1 and S2). The analysis showed that the sEVs from si-EGFR transfected NSCLC cells contained around 20% EGFR expression compared to sEVs secreted from untreated parental cells (Figure S1C, EGFR expression related to CD9 marker). For the HEK 293T cell line instead, the results revealed clearly elevated CD63 expression levels on the EV surface, with detected CD63 mean fluorescence intensities on CD63eGFP sEVs being approximately 80% higher compared to the parental wild type sEVs (Figure S2B) and no detectable EGFR expression on HEK 293T sEVs (data not shown). The sensor responses for the different EGFR and CD63 followed the expected trends (Figure 5), confirming the possibility to detect changes in the expression level of cells via sEV analysis in our sensor. Particularly, a signal of ~3.2 mV was recorded for sEVs derived from parental EGFR-expressing NSCLC cells, and ~1 mV was detected for sEVs derived from si-EGFR


DOI: 10.1021/acssensors.9b00418
ACS Sens. 2019, 4, 1399−1408

NSCLC cells (Figure 5A). An 80% suppression of EGFR expression level, as estimated by WB, produced a change of 2.2 mV in the electrokinetic sensor, which is more than an order of magnitude higher than the minimum measurable signal (~0.2 mV). In the case of HEK 293T sEVs, CD63eGFP-over-expressing sEVs showed a signal of ~7.5 mV and parental sEVs showed a signal of ~1.7 mV (Figure 5B), suggesting that an increase in CD63 expression by 80% led to almost 4-fold increase in the sensor response. Hence, these results illustrate that the developed sensor holds capacity to detect different expression levels of targets in EVs and thereby will allow for heterogeneity of EVs in a biological sample to be monitored.

## DISCUSSION

**Electrokinetic Detection of EVs.** The measurement of streaming potential ($V_s$) and $I_s$is a well-established method for surface characterizations[40,50] and has also been used for detection of specific target molecules, such as proteins, DNA, and so on.[33−35,51] In general, the association/dissociation of charged species on an electrochemically active surface leads to a change in $\zeta^*$ or kinetic potential. In a microfluidic channel, this change can be monitored by measuring $I_s$or $V_s$. The theoretical interpretation of the results mostly relies on the hydrodynamic model[36,52] that considers the damping of convection currents of ions in the vicinity of the adsorbed layer. The model has been successfully used for the interpretation of a range of experimental results on a particle covered surface, including polymeric particles, polyelectrolytes, and silica particles.[36,37,52,53] Both the theoretical and the experimental investigations[36,37,52,53] show a clear and strong dependence of the surface $\zeta^*$ on the particle size, demonstrating that larger particles induce stronger changes in the measured $I_s$ or $V_s$. In addition, for a considerable fraction of the surface coverage, the response remains linear.[37] Both of these features make the electrokinetic measurement technique a suitable platform for sensitive analysis of larger bioanalytes such as EVs. A theoretical analysis presented in the Supporting Information (Section S4) clearly shows a much stronger signal arising from larger particles. The main objective of this study is to exploit this advantage for profiling of sEV surface markers. As seen in Figure 2, the interaction of sEVs with the immobilized anti-EGFR affibody induces a strong change in the $\zeta^*$ compared to the control measurements. Clearly, the results indicate that the method is suitable for both real-time and end-point measurements. Analysis from a low sample volume, as demonstrated with the end-point approach, is preferable for EV analysis in body fluids in general and in cancer diagnostics in particular.[20,54] The required sample volume can be further minimized with microfabricated channels of smaller dimensions than the commercial capillaries.

**Selectivity and Reproducibility of Detection.** The selective detection of sEV surface markers, a key requirement for practical applications, has been evaluated by both electrical and optical approaches (Figures 2B and S2C). It is known that non-specific adsorption and cross-reactivity is a major concern in biomolecular recognition, particularly when dealing with complex biological samples such as EVs containing a large number of proteins and lipid. However, the extent of such cross-reactivity depends on a number of parameters, including the type of the affinity probes, the constellation of surface markers, and their relative affinities with the immobilized probes as well as the local electrolyte environment. A detailed investigation on such cross-reactivity is, however, beyond the scope of the present investigation and therefore has not been accounted for in the analysis. Nevertheless, the prospect of specific surface maker detection has been validated in different ways, which include non-specific binding and the reactivity with control sample isolated from EV-depleted medium. When analyzing the influence of such undesirable responses, the results clearly suggested that the sensor specifically detected sEVs by their surface proteins and that only a small influence arose from the other undesirable interactions (Figure 2B). The detection selectivity was further validated by optical investigations (Figure S2C). As shown, the fluorescence images of the sensor and the control capillary also supported the results obtained with the electrical measurement. Further evidence on target specificity may be obtained from the investigation involving EVs with artificially altered contents of EGFR and CD63. In both cases, the signal showed the expected trend, thereby validating a reasonable specificity of the interaction. In addition to the specificity, the reproducibility of the measurements was evaluated by repeated measurements that showed low SDs, which in most cases were below 10% of the overall signal.

**Detection Time and Sensitivity.** As widely discussed in the context of biosensors, the mass transport to the sensor surface plays a dominant role in sensor design.[55,56] This issue is of particular concern for larger analytes such as EVs, in comparison to other common biomarkers, e.g., proteins, DNAs, and RNAs. For such a large species, a slower mass transport rate is expected, due to the smaller diffusion coefficient. In addition, low abundance of sEVs in body fluids (<pM),[20] makes their detection quite challenging without elaborate sample enrichment steps or appropriate approaches that can overcome the diffusion-limited transport.[17,29] Furthermore, mere proximity to the surface does not ensure an interaction with the immobilized affinity reagents, as a large fraction of EVs may eventually bounce back from the surface without any or little interaction.[57] Indeed, the use of sample enrichment or improved mass transport methods could dramatically enhance the performances of the presented sensing method. However, the purpose of this study is to report on the sensing principle itself, which has rarely been used for specific biodetection and, to the best of our knowledge, has never been applied for the detection and profiling of EVs. As evident from the results, the electrokinetic method can enable profiling of sEV surface proteins in less than 2 h with a particle sensitivity of $2.8 \times 10^8$ particles/mL. A theoretical analysis as presented in Figure 4B clearly suggests a very low surface coverage, indicating sufficient room for further improvement of the sensitivity. A similar analysis also reveals that the minimum measurable signal of ~0.2 mV (Figure 2D) represents a surface coverage of only 0.04% of the total surface area, indicating a very high surface sensitivity of the proposed method. Considering that the average number of sEVs in biological samples ranges from $1 \times 10^8$ to $3 \times 10^{12}$ EVs/mL, including those from plasma of cancer patients,[20,58,59] the sensor in its current form may already be sufficient for many clinical applications.[54] The sensitivity can be further enhanced by optimizing the channel dimension as discussed in the Supporting Information (Section S5). In addition, several sample-pre-enrichment strategies are available,[60,61] which can be integrated with the proposed method allowing for quick and sensitive detection directly from body fluids. Yet it remains to be analyzed further in EVs isolated from plasma of cancer


DOI: 10.1021/acssensors.9b00418
ACS Sens. 2019, 4, 1399−1408

patients and healthy donors, where the target of the affinity probe is monitored also by alternative methods.

**Profiling of EV Surface Markers.** The capacity of a sensor to profile the sEV surface protein expression is of utmost importance for clinical application. Studies have suggested that, in the context of tumor cell derived EVs, the expression level of certain surface markers may change during cancer treatment, reflecting tumor response.[47] In most practical cases, one only needs to compare the qualitative expression level of a marker among different populations, e.g., between cancer patients and healthy controls, or between patients at different stages of treatment. In such cases, one can directly compare the sensor response for a particular surface marker among different samples and this has been a popular approach for EV profiling.[20,27] As presented in Figure 3A, the proposed method is capable of measuring different EV surface markers for potential application in the qualitative comparison of expression levels among various samples. The proposed technique also offers a reasonably good sensitivity to a change in surface marker expression level, as presented in Figure 5. Although the influence of multivalent type interactions on the affinity constant of a target may be quite significant,[16,62] in most practical cases, a linear dependence of the expression level on the sensor response is assumed.[16,18] Such an assumption, in addition to the fact that the proposed method can reliably measure a minimum signal of ∼0.2 mV (Figure 2D), indicates a detection sensitivity equivalent to ∼10% of the normal expression of EGFR in NSCLC H1975 sEVs and ∼3% of normal expression of CD63 in HEK 293T sEVs. We emphasize here that the above analysis is only for indicative purpose, as many parameters such as the size distribution of the EVs, the charge distribution, and the protein profiles on EV surfaces may strongly influence the sensitivity of the sensor. Nevertheless, the evidence presented here clearly suggests the prospect of highly sensitive quantitative protein expression profiling of EVs by the proposed method.

## CONCLUSIONS

In conclusion, an affinity-based electrokinetic sensor for rapid one-step detection and protein expression profiling of sEVs is presented. The technique relies on a streaming current measurement, which is widely used for sensitive surface characterization. The proposed method was validated by detecting NSCLC and HEK 293T cell-derived sEVs targeting EGFR, CD63, and CD9 surface markers. The specificity of target detection was evaluated by simultaneous electrical and optical investigations, revealing a high degree of target selectivity, which was achieved through immobilization of target-specific affinity reagents. Furthermore, repeated measurements demonstrated good reproducibility with standard deviations below 10% of the overall signals, for most cases. An experimental calibration plot revealed a sensitivity of ∼0.4 pM for 2 h of sample incubation, which, however, represented a surface coverage of ∼0.04% only, indicating an extremely high sensitivity toward the surface coverage. The efficacy of the method to perform semiquantitative analysis of sEV surface protein content was also analyzed by using sEV samples containing artificially altered expression levels of EGFR and CD63. The measurements revealed that the method can reliably detect changes in expression levels of important surface markers with high sensitivity, in some cases reaching ∼3% of their normal expression. Upon further optimization of the microcapillary sensor, e.g., by reducing the diameter or length, the sensitivity of the method may be significantly improved, allowing measurements at lower concentrations.

## ASSOCIATED CONTENT

### Supporting Information

The Supporting Information is available free of charge on the ACS Publications website at DOI: 10.1021/acssensors.9b00418.

Detailed description of capillary surface functionalization, standard sEV isolation and characterization protocols, NSCLC H1975 sEV and HEK 293T sEV characterizations, effect of buffer ionic strength: NTA data of sEVs stored in 1 × and 0.1 × PBS, analysis of the surface coverage, and effect of the capillary diameter on the sensor performance (PDF)

## AUTHOR INFORMATION


### Corresponding Author

*E-mail: apurba.dev@angstrom.uu.se.

### ORCID

Sara Cavallaro: 0000-0002-5077-3218

Apurba Dev: 0000-0002-6235-2891


### Notes

The authors declare no competing financial interest.

## ACKNOWLEDGMENTS

The entire study was supported by a grant from the Erling Persson Family Foundation. A.D. and S.S.S. acknowledge also the grant funded by the Swedish Research Council (Contract No. 621-2014-5591). The tumor biology part conducted by P.H., K.V., and R.L. was also supported by Swedish Cancer Society (Grant Nos. CAN 2015/401 and CAN 2018/597), the Stockholm Cancer Society (Grant Nos. 171123, 161283, 154102, and 174093), and the Stockholm County Council (Grant Nos. 20160287 and 20180404) and Karolinska FOUU funding. The SELA laboratory is supported by VR-Med and SSF-IRC. A.G. is an International Society for Advancement of Cytometry (ISAC) Marylou Ingram Scholar. We acknowledge the work by Metka Novak and Msc Vasiliki Arapi on purification and characterization of the sEVs from NSCLC cells. Additionally, we acknowledge the contribution of Ingemar Petermann of RISE Acreo.

## REFERENCES


(1) Whiteside, T. L. The potential of tumor-derived exosomes for noninvasive cancer monitoring. *Expert Rev. Mol. Diagn.* **2015**, *15* (10), 1293−1310.

(2) El Andaloussi, S.; Maeger, I.; Breakefield, X. O.; Wood, M. J. A. Extracellular vesicles: biology and emerging therapeutic opportunities. *Nat. Rev. Drug Discovery* **2013**, *12* (5), 347−357.

(3) Vader, P.; Breakefield, X. O.; Wood, M. J. A. Extracellular vesicles: emerging targets for cancer therapy. *Trends Mol. Med.* **2014**, *20* (7), 385−393.

(4) Lotvall, J.; Hill, A. F.; Hochberg, F.; Buzas, E. I.; Di Vizio, D.; Gardiner, C.; Gho, Y. S.; Kurochkin, I. V.; Mathivanan, S.; Quesenberry, P.; Sahoo, S.; Tahara, H.; Wauben, M. H.; Witwer, K. W.; Thery, C. Minimal experimental requirements for definition of extracellular vesicles and their functions: a position statement from the International Society for Extracellular Vesicles. *J. Extracell. Vesicles* **2014**, *3* (1−6), 26913.

(5) Thery, C.; Witwer, K. W.; Aikawa, E.; Alcaraz, M. J.; Anderson, J. D.; Andriantsitohaina, R.; Antoniou, A.; Arab, T.; Archer, F.; Atkin-Smith, G. K.; et al. Minimal information for studies of extracellular




DOI: 10.1021/acssensors.9b00418
*ACS Sens.* 2019, 4, 1399−1408

vesicles 2018 (MISEV2018): a position statement of the International Society for Extracellular Vesicles and update of the MISEV2014 guidelines. *J. Extracell. Vesicles* **2018**, *7* (1), 1535750.
(6) Becker, A.; Thakur, B. K.; Weiss, J. M.; Kim, H. S.; Peinado, H.; Lyden, D. Extracellular Vesicles in Cancer: Cell-to-Cell Mediators of Metastasis. *Cancer Cell* **2016**, *30* (6), 836−848.
(7) Peinado, H.; Zhang, H. Y.; Matei, I. R.; Costa-Silva, B.; Hoshino, A.; Rodrigues, G.; Psaila, B.; Kaplan, R. N.; Bromberg, J. F.; Kang, Y. B.; Bissell, M. J.; Cox, T. R.; Giaccia, A. J.; Erler, J. T.; Hiratsuka, S.; Ghajar, C. M.; Lyden, D. Pre-metastatic niches: organ-specific homes for metastases. *Nat. Rev. Cancer* **2017**, *17* (5), 302−317.
(8) Cui, S. H.; Cheng, Z. A.; Qin, W. X.; Jiang, L. Y. Exosomes as a liquid biopsy for lung cancer. *Lung Cancer* **2018**, *116*, 46−54.
(9) Halvaei, S.; Daryani, S.; Eslami-S, Z.; Samadi, T.; Jafarbeik-Iravani, N.; Bakhshayesh, T. O.; Majidzadeh-A, K.; Esmaeili, R. Exosomes in Cancer Liquid Biopsy: A Focus on Breast Cancer. *Mol. Ther.–Nucleic Acids* **2018**, *10*, 131−141.
(10) Boukouris, S.; Mathivanan, S. Exosomes in bodily fluids are a highly stable resource of disease biomarkers. *Proteomics: Clin. Appl.* **2015**, *9* (3−4), 358−367.
(11) Palmieri, V.; Lucchetti, D.; Gatto, I.; Maiorana, A.; Marcantoni, M.; Maulucci, G.; Papi, M.; Pola, R.; De Spirito, M.; Sgambato, A. Dynamic light scattering for the characterization and counting of extracellular vesicles: a powerful noninvasive tool. *J. Nanopart. Res.* **2014**, *16* (9), 2583.
(12) Wiklander, O. P. B.; Bostancioglu, R. B.; Welsh, J. A.; Zickler, A. M.; Murke, F.; Corso, G.; Felldin, U.; Hagey, D. W.; Evertsson, B.; Liang, X. M.; Gustafsson, M. O.; Mohammad, D. K.; Wiek, C.; Hanenberg, H.; Bremer, M.; Gupta, D.; Bjornstedt, M.; Giebel, B.; Nordin, J. Z.; Jones, J. C.; El Andaloussi, S.; Gorgens, A. Systematic Methodological Evaluation of a Multiplex Bead-Based Flow Cytometry Assay for Detection of Extracellular Vesicle Surface Signatures. *Front. Immunol.* **2018**, *9*, 1326.
(13) Larssen, P.; Wik, L.; Czarnewski, P.; Eldh, M.; Lof, L.; Ronquist, K. G.; Dubois, L.; Freyhult, E.; Gallant, C. J.; Oelrich, J.; Larsson, A.; Ronquist, G.; Villablanca, E. J.; Landegren, U.; Gabrielsson, S.; Kamali-Moghaddam, M. Tracing Cellular Origin of Human Exosomes Using Multiplex Proximity Extension Assays. *Mol. Cell. Proteomics* **2017**, *16* (3), 502−511.
(14) Yoshioka, Y.; Konishi, Y.; Kosaka, N.; Katsuda, T.; Kato, T.; Ochiya, T. Comparative marker analysis of extracellular vesicles in different human cancer types. *J. Extracell. Vesicles* **2013**, *2*, 20424.
(15) Lu, Q.; Zhang, J.; Allison, R.; Gay, H.; Yang, W. X.; Bhowmick, N. A.; Frelix, G.; Shappell, S.; Chen, Y. H. Identification of Extracellular delta-Catenin Accumulation for Prostate Cancer Detection. *Prostate* **2009**, *69* (4), 411−418.
(16) Im, H.; Shao, H. L.; Park, Y. I.; Peterson, V. M.; Castro, C. M.; Weissleder, R.; Lee, H. Label-free detection and molecular profiling of exosomes with a nano-plasmonic sensor. *Nat. Biotechnol.* **2014**, *32* (5), 490−495.
(17) Vaidyanathan, R.; Naghibosadat, M.; Rauf, S.; Korbie, D.; Carrascosa, L. G.; Shiddiky, M. J. A.; Trau, M. Detecting Exosomes Specifically: A Multiplexed Device Based on Alternating Current Electrohydrodynamic Induced Nanoshearing. *Anal. Chem.* **2014**, *86* (22), 11125−11132.
(18) Zhao, Z.; Yang, Y.; Zeng, Y.; He, M. A microfluidic ExoSearch chip for multiplexed exosome detection towards blood-based ovarian cancer diagnosis. *Lab Chip* **2016**, *16* (3), 489−496.
(19) Jorgensen, M. M.; Baek, R.; Varming, K. Potentials and capabilities of the Extracellular Vesicle (EV) Array. *J. Extracell. Vesicles* **2015**, *4* (1−8), 26048.
(20) Sina, A. A. I.; Vaidyanathan, R.; Dey, S.; Carrascosa, L. G.; Shiddiky, M. J. A.; Trau, M. Real time and label free profiling of clinically relevant exosomes. *Sci. Rep.* **2016**, *6*, 30460.
(21) Kanwar, S. S.; Dunlay, C. J.; Simeone, D. M.; Nagrath, S. Microfluidic device (ExoChip) for on-chip isolation, quantification and characterization of circulating exosomes. *Lab Chip* **2014**, *14* (11), 1891−1900.
(22) Dudani, J. S.; Gossett, D. R.; Tse, H. T. K.; Lamm, R. J.; Kulkarni, R. P.; Di Carlo, D. Rapid inertial solution exchange for enrichment and flow cytometric detection of microvesicles. *Biomicrofluidics* **2015**, *9* (1), No. 014112.
(23) Guo, S. C.; Tao, S. C.; Dawn, H. Microfluidics-based on-a-chip systems for isolating and analysing extracellular vesicles. *J. Extracell. Vesicles* **2018**, *7* (1), 1508271.
(24) Wang, Z. X.; Wu, H. J.; Fine, D.; Schmulen, J.; Hu, Y.; Godin, B.; Zhang, J. X. J.; Liu, X. W. Ciliated micropillars for the microfluidic-based isolation of nanoscale lipid vesicles. *Lab Chip* **2013**, *13* (15), 2879−2882.
(25) Contreras-Naranjo, J. C.; Wu, H. J.; Ugaz, V. M. Microfluidics for exosome isolation and analysis: enabling liquid biopsy for personalized medicine. *Lab Chip* **2017**, *17* (21), 3558−3577.
(26) Maeki, M.; Kimura, N.; Sato, Y.; Harashima, H.; Tokeshi, M. Advances in microfluidics for lipid nanoparticles and extracellular vesicles and applications in drug delivery systems. *Adv. Drug Delivery Rev.* **2018**, *128*, 84−100.
(27) Jeong, S.; Park, J.; Pathania, D.; Castro, C. M.; Weissleder, R.; Lee, H. Integrated Magneto-Electrochemical Sensor for Exosome Analysis. *ACS Nano* **2016**, *10* (2), 1802−1809.
(28) Zhou, Q.; Rahimian, A.; Son, K.; Shin, D. S.; Patel, T.; Revzin, A. Development of an aptasensor for electrochemical detection of exosomes. *Methods* **2016**, *97*, 88−93.
(29) Doldan, X.; Fagundez, P.; Cayota, A.; Laiz, J.; Tosar, J. P. Electrochemical Sandwich Immunosensor for Determination of Exosomes Based on Surface Marker-Mediated Signal Amplification. *Anal. Chem.* **2016**, *88* (21), 10466−10473.
(30) Zhou, Y. G.; Mohamadi, R. M.; Poudineh, M.; Kermanshah, L.; Ahmed, S.; Safaei, T. S.; Stojcic, J.; Nam, R. K.; Sargent, E. H.; Kelley, S. O. Interrogating Circulating Microsomes and Exosomes Using Metal Nanoparticles. *Small* **2016**, *12* (6), 727−732.
(31) Wang, S.; Zhang, L. Q.; Wan, S.; Cansiz, S.; Cui, C.; Liu, Y.; Cai, R.; Hong, C. Y.; Teng, I. T.; Shi, M. L.; Wu, Y.; Dong, Y. Y.; Tan, W. H. Aptasensor with Expanded Nucleotide Using DNA Nanotetrahedra for Electrochemical Detection of Cancerous Exosomes. *ACS Nano* **2017**, *11* (4), 3943−3949.
(32) Adamczyk, Z.; Sadlej, K.; Wajnryb, E.; Nattich, M.; Ekiel-Jezewska, M. L.; Blawzdziewicz, J. Streaming potential studies of colloid, polyelectrolyte and protein deposition. *Adv. Colloid Interface Sci.* **2010**, *153* (1−2), 1−29.
(33) Dev, A.; Horak, J.; Kaiser, A.; Yuan, X. C.; Perols, A.; Bjork, P.; Karlstrom, A. E.; Kleimann, P.; Linnros, J. Electrokinetic effect for molecular recognition: A label-free approach for real-time biosensing. *Biosens. Bioelectron.* **2016**, *82*, 55−63.
(34) Koch, S.; Woias, P.; Meixner, L. K.; Drost, S.; Wolf, H. Protein detection with a novel ISFET-based zeta potential analyzer. *Biosens. Bioelectron.* **1999**, *14* (4), 413−421.
(35) Martins, D. C.; Chu, V.; Prazeres, D. M. F.; Conde, J. P. Electrical detection of DNA immobilization and hybridization by streaming current measurements in microchannels. *Appl. Phys. Lett.* **2011**, *99* (18), 183702.
(36) Zembala, M.; Adamczyk, Z. Measurements of streaming potential for mica covered by colloid particles. *Langmuir* **2000**, *16* (4), 1593−1601.
(37) Michelmore, A. P.; Hayes, R. A. The effect of deposition of negatively charged particles on the electrokinetic behaviour of oppositely charged surfaces. *PhysChemComm* **2000**, *3* (6), 24−28.
(38) Tolmachev, V.; Rosik, D.; Wallberg, H.; Sjoberg, A.; Sandstrom, M.; Hansson, M.; Wennborg, A.; Orlova, A. Imaging of EGFR expression in murine xenografts using site-specifically labelled anti-EGFR 111In-DOTA-Z EGFR:2377 Affibody molecule: aspect of the injected tracer amount. *Eur. J. Nucl. Med. Mol. Imaging* **2010**, *37* (3), 613−22.
(39) Hunter, R. J. *Zeta potential in colloid science: Principles and applications*; Academic Press: London, 1988.
(40) Kirby, B. J.; Hasselbrink, E. F. Zeta potential of microfluidic substrates: 1. Theory, experimental techniques, and effects on separations. *Electrophoresis* **2004**, *25* (2), 187−202.


DOI: 10.1021/acssensors.9b00418
*ACS Sens.* 2019, 4, 1399−1408

(41) Pao, W.; Miller, V. A.; Politi, K. A.; Riely, G. J.; Somwar, R.; Zakowski, M. F.; Kris, M. G.; Varmus, H. Acquired resistance of lung adenocarcinomas to gefitinib or erlotinib is associated with a second mutation in the EGFR kinase domain. *PLos Med.* **2005**, *2* (3), e73.
(42) Corso, G.; Mager, I.; Lee, Y.; Gorgens, A.; Bultema, J.; Giebel, B.; Wood, M. J. A.; Nordin, J. Z.; Andaloussi, S. E. L. Reproducible and scalable purification of extracellular vesicles using combined bind-elute and size exclusion chromatography. *Sci. Rep.* **2017**, *7*, 11561.
(43) Koliha, N.; Wiencek, Y.; Heider, U.; Jungst, C.; Kladt, N.; Krauthauser, S.; Johnston, I. C. D.; Bosio, A.; Schauss, A.; Wild, S. A novel multiplex bead-based platform highlights the diversity of extracellular vesicles. *J. Extracell. Vesicles* **2016**, *5*, 29975.
(44) Kobayashi, S.; Boggon, T. J.; Dayaram, T.; Janne, P. A.; Kocher, O.; Meyerson, M.; Johnson, B. E.; Eck, M. J.; Tenen, D. G.; Halmos, B. EGFR mutation and resistance of non-small-cell lung cancer to gefitinib. *N. Engl. J. Med.* **2005**, *352* (8), 786−792.
(45) Ochieng, J.; Pratap, S.; Khatua, A. K.; Sakwe, A. M. Anchorage-independent growth of breast carcinoma cells is mediated by serum exosomes. *Exp. Cell Res.* **2009**, *315* (11), 1875−1888.
(46) Loock, H. P.; Wentzell, P. D. Detection limits of chemical sensors: Applications and misapplications. *Sens. Actuators, B* **2012**, *173*, 157−163.
(47) Verma, M.; Lam, T. K.; Hebert, E.; Divi, R. L. Extracellular vesicles: potential applications in cancer diagnosis, prognosis, and epidemiology. *BMC Clin. Pathol.* **2015**, *15*, 6.
(48) Li, W. H.; Li, C. Y.; Zhou, T.; Liu, X. H.; Liu, X. N.; Li, X. H.; Chen, D. X. Role of exosomal proteins in cancer diagnosis. *Mol. Cancer* **2017**, *16*, 145.
(49) Jakobsen, K. R.; Paulsen, B. S.; Baek, R.; Varming, K.; Sorensen, B. S.; Jorgensen, M. M. Exosomal proteins as potential diagnostic markers in advanced non-small cell lung carcinoma. *J. Extracell. Vesicles* **2015**, *4*, 26659.
(50) Kirby, B. J.; Hasselbrink, E. F. Zeta potential of microfluidic substrates: 2. Data for polymers. *Electrophoresis* **2004**, *25* (2), 203−213.
(51) Glad, C.; Sjodin, K.; Mattiasson, B. STREAMING POTENTIAL - A GENERAL AFFINITY SENSOR. *Biosensors* **1986**, *2* (2), 89−100.
(52) Adamczyk, Z.; Warszynski, P.; Zembala, M. Influence of adsorbed colloid particles on streaming potential. *Bull. Polym. Acad. Sci.-Chem.* **1999**, *47* (3), 239−258.
(53) Zembala, M. Electrokinetics of heterogeneous interfaces. *Adv. Colloid Interface Sci.* **2004**, *112* (1−3), 59−92.
(54) de Vrij, J.; Maas, S. L. N.; van Nispen, M.; Sena-Esteves, M.; Limpens, R. W. A.; Koster, A. J.; Leenstra, S.; Lamfers, M. L.; Broekman, M. L. D. Quantification of nanosized extracellular membrane vesicles with scanning ion occlusion sensing. *Nanomedicine* **2013**, *8* (9), 1443−1458.
(55) Sheehan, P. E.; Whitman, L. J. Detection limits for nanoscale biosensors. *Nano Lett.* **2005**, *5* (4), 803−807.
(56) Squires, T. M.; Messinger, R. J.; Manalis, S. R. Making it stick: convection, reaction and diffusion in surface-based biosensors. *Nat. Biotechnol.* **2008**, *26* (4), 417−426.
(57) Yang, Y. T.; Shen, G. X.; Wang, H.; Li, H. X.; Zhang, T.; Tao, N. J.; Ding, X. T.; Yu, H. Interferometric plasmonic imaging and detection of single exosomes. *Proc. Natl. Acad. Sci. U. S. A.* **2018**, *115* (41), 10275−10280.
(58) Huang, X. Y.; Yuan, T. Z.; Tschannen, M.; Sun, Z. F.; Jacob, H.; Du, M. J.; Liang, M. H.; Dittmar, R. L.; Liu, Y.; Liang, M. Y.; Kohli, M.; Thibodeau, S. N.; Boardman, L.; Wang, L. Characterization of human plasma-derived exosomal RNAs by deep sequencing. *BMC Genomics* **2013**, *14*, 319.
(59) Ricklefs, F. L.; Maire, C. L.; Reimer, R.; Dührsen, L.; Kolbe, K.; Holz, M.; Schneider, E.; Rissiek, A.; Babayan, A.; Hille, C.; et al. Imaging flow cytometry facilitates multiparametric characterization of extracellular vesicles in malignant brain tumours. *J. Extracell. Vesicles* **2019**, *8* (1), 1588555.
(60) Ku, A.; Lim, H. C.; Evander, M.; Lilja, H.; Laurell, T.; Scheding, S.; Ceder, Y. Acoustic Enrichment of Extracellular Vesicles from Biological Fluids. *Anal. Chem.* **2018**, *90* (13), 8011−8019.
(61) Li, Z.; Hu, C.; Jia, J.; Xia, Y.; Xie, H.; Shen, M.; Huang, R.; He, L.; Liu, C.; Wang, S.; Chen, B.; He, N. Establishment and Evaluation of a Simple Size-Selective Method for Exosome Enrichment and Purification. *J. Biomed. Nanotechnol.* **2019**, *15* (5), 1090−1096.
(62) Tassa, C.; Duffner, J. L.; Lewis, T. A.; Weissleder, R.; Schreiber, S. L.; Koehler, A. N.; Shaw, S. Y. Binding Affinity and Kinetic Analysis of Targeted Small Molecule-Modified Nanoparticles. *Bioconjugate Chem.* **2010**, *21* (1), 14−19.


DOI: 10.1021/acssensors.9b00418
*ACS Sens.* 2019, 4, 1399−1408